Earth and Planetary Science Letters xxx (2008) xxx-xxx

Contents lists available at ScienceDirect

Earth and Planetary Science Letters

journal homepage: www.elsevier.com/locate/epsl

The rate of oceanic detachment faulting at Atlantis Bank, SW Indian Ridge

A. Graham Baines *, Michael J. Cheadle, Barbara E. John, Joshua J. Schwartz [1]

Department of Geology and Geophysics, University of Wyoming, Laramie, Wyoming 82071, USA

ARTICLE INFO

Article history:
Received 4 March 2008
Received in revised form 28 May 2008
Accepted 11 June 2008
Available online xxxx

Editor: R.D. van der Hilst

Keywords:
oceanic core-complexes
detachment faulting
Southwest Indian Ridge
Atlantis II Transform
magnetic anomalies
U–Pb dating

ABSTRACT

The rates of slip on oceanic detachment faults and how those rates compare to sea-floor spreading rates constitute fundamental data required to constrain how oceanic core-complexes form and their role during crustal accretion. We combine sea-surface magnetic data, with the magnetic polarity of shallow-core samples and Pb/U SHRIMP ages of igneous zircon to determine the time-averaged half-spreading rate during oceanic detachment faulting at Atlantis Bank, 100 km south of the ultraslow-spreading Southwest Indian Ridge (SWIR). The Pb/U zircon ages correlate well with the magnetic ages and so highlight that magmatic accretion and faulting were coeval for over 2 Myr, creating and exposing a >1.5-km-thick layer of gabbro for >35 km parallel-to-spreading. We use bivariate linear regression of distance–age data and forward modeling of magnetic anomaly data to calculate a half-spreading rate during detachment faulting of 14.1 + 1.8/− 1.5 km/Myr (95% confidence limits). When integrated with regional constraints on spreading history, we note that detachment faulting coincided with a short-lived regional increase in the full-spreading rate along the SWIR and, for the ridge segment containing Atlantis Bank, spreading was highly asymmetric with ~80% of plate-motion accommodated by detachment faulting. Consequently, the detachment fault effectively formed the plate-boundary at the surface in this spreading segment. Highly asymmetric spreading was confined to the spreading segment containing Atlantis Bank and to the duration of detachment faulting. So the ridge segment containing Atlantis Bank migrated northward relative to its symmetrically spreading eastern neighbour, such that the intervening non-transform discontinuity shortened. We suggest that the highly asymmetric spreading may be a characteristic feature of oceanic detachment faulting, an inference supported by more poorly constrained half-spreading rates determined at several other oceanic core-complexes.

1. Introduction

At slow- and ultraslow-spreading mid-ocean ridges large offset (>10 km) normal fault systems, referred to as oceanic detachment faults, expose gabbro and peridotite at the sea-floor in domal massifs termed 'oceanic core-complexes' (Cann et al., 1997; Blackman et al., 1998; Tucholke et al., 1998; Escartin et al., 2003; Searle et al., 2003; Smith et al., 2006). Active oceanic detachment faults root in the axial valley of these mid-ocean ridges so slip on these faults may accommodate a significant component of sea-floor spreading, such that these faults can be considered an integral part of the plate-boundary system (Fig. 1). Although many authors have assumed symmetric sea-floor spreading rates during detachment faulting (Tucholke et al., 2001, 1998; Escartin et al., 2003; Buck et al., 2005); there is evidence for both short- and long-lived asymmetric spreading rates at slow- and ultraslow-spreading mid-ocean ridges (Allerton et al., 2000; Hosford et al., 2003). To test the assumption of symmetric spreading during slip on oceanic detachment faults and improve our understanding of the dynamics and conditions that form these fault systems, accurate determinations of half-spreading rates during detachment faulting are needed. To date, slip-rates on these faults have been inferred solely from the interpretation of sea-surface magnetic anomaly data. However, magnetic anomalies are often unclear over oceanic core-complexes, most likely because core-complexes expose sometimes weakly magnetic lower crustal and mantle rocks rather than basalt. Consequently, the few spreading rates determined have been poorly constrained (Schulz et al., 1988; Searle et al., 2003). Recently, radiometric dating techniques have been used for the first time to accurately date oceanic crust across an oceanic core-complex (John et al., 2004; Schwartz et al., 2005), and the opportunity now exists to use these data to provide independent constraints on half-spreading rates during detachment faulting. Here we combine Pb/U ages from igneous zircon with detailed magnetic data from the Atlantis Bank oceanic core-complex, on the SWIR, to determine the half-spreading rate during detachment faulting. We argue that this spreading rate approximately corresponds to the rate of slip on this oceanic detachment fault (Fig. 1), as intrusion of the exposed gabbros, cooling through the Curie temperature and denudation during detachment faulting were synchronous or

* Corresponding author. Present address: School of Earth and Environmental Sciences, University of Adelaide, Adelaide 5005, Australia.
E-mail address: graham.baines@adelaide.edu.au (A.G. Baines).
[1] Present address: Department of Geological Sciences, University of Alabama, Tuscaloosa, AL 35487 USA.

0012-821X/$ – see front matter © 2008 Elsevier B.V. All rights reserved.
doi:10.1016/j.epsl.2008.06.013

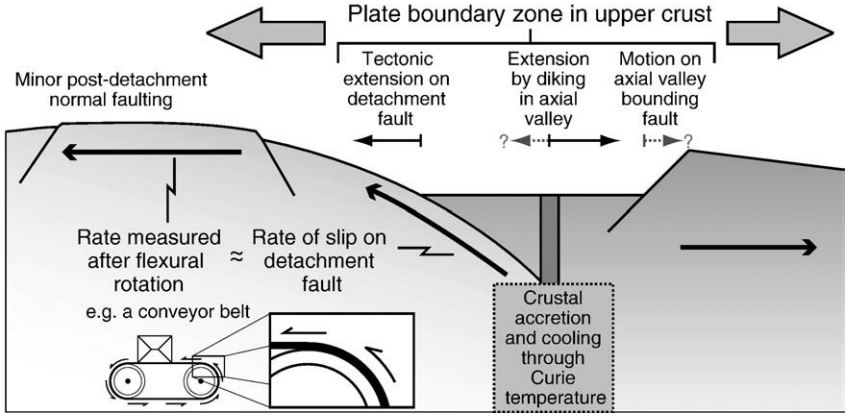

Fig. 1. The accommodation of sea-floor spreading in the upper crust during detachment faulting. Flexural rotation following denudation on the detachment fault suggests that half-spreading rates determined by magnetic data and absolute ages over a detachment fault will record the original time-averaged rate of slip along the detachment fault prior to rotation.

occurred very rapidly (Dick et al., 2000; Natland and Dick, 2002; John et al., 2004; Miranda, 2006; Coogan et al., 2007). Flexural rotation of the footwall to the detachment fault (Buck, 1988) means that the horizontal half-spreading rate approximates the original rate of slip on the dipping fault system (Fig. 1). We also use regional magnetic data from the surrounding region to place this rate of detachment faulting in a broader plate tectonic context.

2. Regional setting

Atlantis Bank (Fig. 2) is a well-studied oceanic core-complex located on the Antarctic Plate ~100 km south of the axial valley of the ultraslow-spreading SW Indian Ridge (Fig. 2c inset), between the Atlantis II Transform fault (~57°05′E) and a fracture zone associated with a non-transform discontinuity at ~57°40′E (Dick et al., 1991). At Atlantis Bank, detachment faulting exposed relatively evolved gabbros and subsidiary peridotite for at least 35 km parallel-to-spreading (Dick et al., 2000; Matsumoto et al., 2002). Extensive high-temperature crystal plastic textures are observed in gabbros from ODP Hole 735B (Dick et al., 2000) and from the surface of Atlantis Bank (Miranda, 2006), suggesting that deformation was synchronous with or immediately followed gabbro emplacement. Fluid inclusion data from the upper 500 m of core recovered in ODP Hole 735B suggest that intrusion and cooling of gabbros occurred only 1.5–2 km below the sea-floor (Vanko and Stakes,

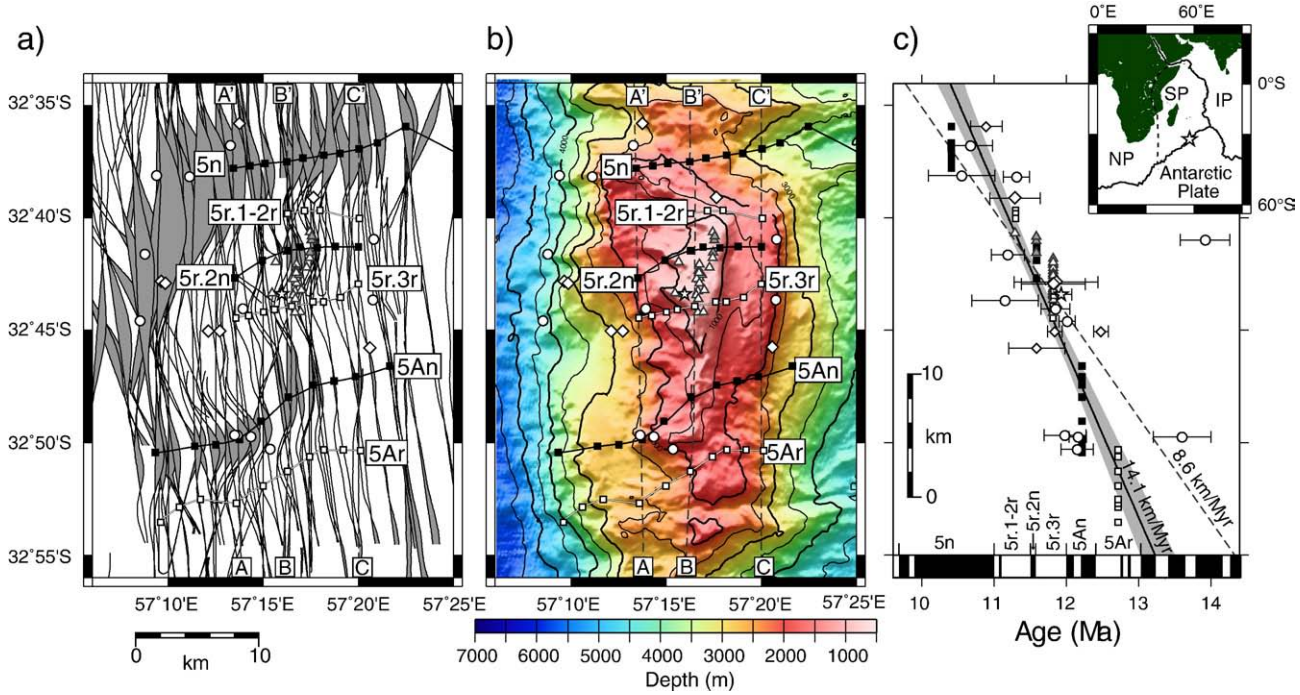

Fig. 2. a) Crustal magnetization plotted along ship tracks over Atlantis Bank. Hand picked isochrons are also plotted: Normal polarity isochrons — thick black lines and reverse polarity isochrons — black and white lines. Also shown are the location of submersible samples (circles), dredge samples (diamonds) and ODP Hole 735B (star) that were dated using the U/Pb method (John et al., 2004; Schwartz et al., 2005). Grey triangles show the location of shallow drill cores whose magnetic polarities were presented by Allerton and Tivey (2001): Solid triangles — normal polarity, open triangles — reverse polarity. b) Shaded bathymetry of Atlantis Bank: symbols as in (a), plus thin black lines — 500 m contours, dashed black lines — profiles used in Fig. 3. c) Latitude versus age for the samples and for the isochrons at the same scale. Symbols are the same as for (a) with the exception of the magnetic data, which are plotted as squares (filled for normal chrons, open for reversed chrons). Also shown are the best-fit bivariate linear regression (thin solid black line), the 95% confidence limits on that line (grey shading), and the average half-spreading rate of 8.6 km/Myr since 20 Ma. Age error bars are only shown for the Pb/U zircon ages. The magnetic polarity timescale is shown as a black and white panel at the bottom and provides an indication of errors for the magnetic ages. Location error for each point is <2 km. Inset shows the location of Atlantis Bank (star): SP — Somalian Plate, NP — Nubian Plate, IP — Indian Plate (after Horner-Johnson et al., 2005).

Please cite this article as: Baines, A.G., et al., The rate of oceanic detachment faulting at Atlantis Bank, SW Indian Ridge Earth and Planetary Science Letters (2008), doi:10.1016/j.epsl.2008.06.013

1991), and paleomagnetic data implies 19±5° footwall rotation for temperatures below the Curie temperature (<580 °C: Kikawa and Pariso, 1991; Worm, 2001; Natland and Dick, 2002). Although this implies relatively low degrees of rotation, tectonic rotation above the Curie temperature at Atlantis Bank is unconstrained, so we cannot preclude greater tectonic rotation (e.g. Garcés and Gee, 2007) that may be more consistent with a rolling-hinge model for detachment faulting (Buck, 1988; deMartin et al., 2007).

Atlantis Bank is a 40 km by 20 km bathymetric massif, elongate in the N–S direction, that rises to 718-m depth (Fig. 2). The anomalous uplift of this platform was partly due to flexural uplift following extension on the outward dipping moderate–high-angle normal faults that bound it (Baines et al., 2003). The anomalous elevation of Atlantis Bank has two major benefits for this study; it reduces attenuation of the magnetic anomaly observed at sea-level providing relatively high-resolution data and has made Atlantis Bank easily accessible for drilling and submersible sampling yielding a sample suite that has been absolutely dated (John et al., 2004; Schwartz et al., 2005). These factors provide an unprecedented opportunity to investigate the kinematic evolution of this core-complex.

3. Data

3.1. Magnetic data

Clear linear magnetic anomalies are observed on sea-surface magnetic anomaly data over Atlantis Bank because the exposed gabbros form a good magnetic source layer (Kikawa and Pariso, 1991; Worm, 2001; Natland and Dick, 2002), and the anomalously shallow bathymetry reduces attenuation of the magnetic anomaly observed at sea level. Correlation of these anomalies to the geomagnetic polarity timescale (Ogg and Smith, 2004) allows us to determine the time-averaged half-spreading rate over the oceanic core-complex. The sea-surface magnetic anomaly data used in this study was collected during cruises by the R/V Robert Conrad in 1987 (Dick et al., 1991), the R/V Karei in 2000 (Hosford et al., 2003), and the R/V Yokosuka in 1998 (Hosford et al., 2003) and 2001 (Baines et al., 2007). Baines et al. (2007) inverted these data for crustal magnetization and anomalies were correlated to the geomagnetic polarity timescale 2004 (GPTS 2004, Ogg and Smith, 2004). Approximately north–south profiles of crustal magnetization were extracted from the gridded solution along the original ship tracks and isochrons were handpicked at peaks or troughs in the crustal magnetization solution and assigned the age at the mid-point of the corresponding polarity epoch (Fig. 2a) (Baines et al., 2007). For this study, we limited ourselves to ten approximately evenly spaced points per isochron over Atlantis Bank to prevent the possibility of these data dominating subsequent calculations of spreading rates that include other data.

Isochrons over Atlantis Bank trend approximately ENE-WSW (average 080°), especially chrons C5r.3r and C5An. This trend is oblique to the E–W trend that would be expected for an orthogonal spreading segment, given the north–south direction of relative plate-motion. Although regionally most isochrons trend approximately east–west, the ENE-WSW trend of isochrons over Atlantis Bank is not particularly unusual for the area (Baines et al., 2007). We note that the observed anomalies are locally consistent with the majority of U–Pb ages, therefore the ENE-WSW trend of the isochrons may be a primary feature reflecting obliquity of the paleo-ridge axis during the formation of Atlantis Bank. Alternative explanations, such as topographic truncation of shallowly south-dipping E–W-trending magnetic polarity boundaries (Allerton and Tivey, 2001) due to major mass wasting on the western flank of Atlantis Bank or sinistral deformation on observed transform-parallel normal faults (Baines et al., 2003), may partially contribute to, but cannot fully account for, the observed ENE-WSW trend of the isochrons.

In addition to the sea-surface magnetic data, estimated magnetic ages based on the magnetic polarity of 23 shallow-core samples drilled across the summit of Atlantis Bank provide additional constraints (Allerton and Tivey, 2001). The shallow cores acquired their magnetic remanence during polarity chrons C5r.1-2r, C5r.2n and C5r.3r. Although it is possible to interpolate magnetic ages of the three cores within the 60 kyr chron C5r.2n based on their position within that chron, attempting similar interpolation for the remaining 20 cores requires using the isochrons identified from sea-surface anomaly data. This would bias the results of later inversions for spreading rate towards that determined from the sea-surface data. So, in order to treat these core data independently and consistently, all the cores were assigned ages corresponding to the mid-point of their respective polarity chrons. Two additional data points were defined that correspond to the boundaries of polarity chron C5r.2n, and are located at the mid-point between neighbouring cores of opposite polarity.

3.2. U/Pb ages

Twenty Pb/U SHRIMP zircon ages have been obtained from undeformed gabbroic rock samples recovered from the footwall of the detachment fault by dredges, manned and unmanned submersible dives (Schwartz et al., 2005), and from ODP Hole 735B (John et al., 2004). These ages independently validate the identified magnetic isochrons and provide further constraints on the spreading rate over Atlantis Bank. The dated samples span a spreading-parallel distance of 25.6 km and range in composition from gabbro to oxide gabbro and magmatic felsic veins (Schwartz et al., 2005). Five of the ages are anomalously old compared to the magnetic data and may represent crystallization in the upper 5–18 km of lithosphere followed by later assimilation into crustal gabbros (Schwartz et al., 2005). Excluding these five anomalous ages, the remaining Pb/U SHRIMP zircon ages range from 10.6–12.2 Ma with 2σ errors of 1–5% (0.1–0.6 Myr). We have calculated spreading rates using all twenty ages, and by excluding the five anomalous samples (Table 1).

4. Calculating half-spreading rates

To determine the half-spreading rate over Atlantis Bank and to quantify the accuracy of that rate, we use two complimentary methods: i) bivariate linear regression of discrete magnetic and U–Pb distance–age data, and ii) iterative forward modeling of individual magnetic anomaly profiles.

4.1. Regression of distance–time data for spreading rate

We calculate half-spreading rates using the linear bivariate regression method (York, 1966). Due to the statistically small sample size and presence of scatter in the data that is not caused by analytical

Table 1
Spreading rates and confidence limits calculated over Atlantis Bank

Distance–age data	Sample size	Raw data			Corrected data[a]		
		Rate	S.E.[b]	95% confidence limits	Rate	S.E.[b]	95% confidence limits
Magnetic data	75	13.8	1.2	+1.8/−1.5	13.2	1.1	+1.7/−1.3
All Pb/U ages	20	14.3	6.9	+15.7/−5.4	14.5	6.2	+14.6/−5.7
Pb/U ages (excluding anomalous ages)[c]	15	14.6	4.4	+9.6/−3.9	15.4	4.7	+11.6/−4.9
Magnetic and all Pb/U ages	95	13.6	1.7	+2.0/−1.9	13.2	1.2	+1.8/−1.8
Magnetic and Pb/U ages (excluding anomalous ages)[c]	90	14.1	1.2	+1.8/−1.5	13.7	1.2	+1.6/−1.3

[a] Corrected for an assumed paleo-ridge orientation of 080°N.
[b] Standard error.
[c] After Schwartz et al. (2005).

Please cite this article as: Baines, A.G., et al., The rate of oceanic detachment faulting at Atlantis Bank, SW Indian Ridge Earth and Planetary Science Letters (2008), doi:10.1016/j.epsl.2008.06.013

error alone, we weight each point equally and determine confidence limits on the rates using the bootstrap method (Efron and Tibshirani, 1994). In this application of the bootstrap method, confidence limits were determined by performing linear bivariate regression for 10,000 randomly defined samples of the original data. Each random sample had the same number of points as the original data set, but the points that comprised the sample were chosen at random such that each point could be selected more than once. The resulting 10,000 spreading rates were used to calculate normalized probability density functions (PDFs) of spreading rate that define the median spreading rate and 95% confidence limits on that rate. When the spreading rate was well-constrained the 95% confidence limits determined by the bootstrap method were equivalent to the standard errors calculated by linear bivariate regression, however when errors were large as is relatively common when determining spreading rates over such short time intervals (e.g. Baines et al., 2007), the bootstrap method revealed significant skew in the PDFs, and thus the confidence limits, that is not revealed by the standard errors. For this reason, we report the results of the bootstrap, as they better reflect the uncertainty in the calculated spreading rates.

4.2. Forward modeling magnetic anomaly profiles

The regression outlined above uses only the discrete handpicked isochrons, however we can objectively assess the results of the regression by modeling the magnetic anomaly profiles themselves. To do this we forward model magnetic anomaly profiles using the method of Parker (1972) for a range of spreading velocities and inferred age at 32°43.4′S (the latitude of ODP Hole 735B) and compare these models to the observed magnetic anomaly profile. This is analogous to iteratively varying the slope (velocity) and intercept (age) of a line on a plot of age against distance to minimize error. To calculate the forward models we assume a 1.5-km-thick magnetic source layer whose upper boundary is defined by the observed bathymetry. Discrete blocks of constant magnetization with vertical boundaries were defined given an input spreading velocity and the geomagnetic polarity timescale 2004 (GPTS 2004: Ogg and Smith, 2004). The blocks are magnetized parallel to a geocentric dipole with magnetizations of ±2 A/m, which approximates the average magnetization of ODP Hole 735B (Shipboard Scientific Party, 1999), and the background field defined by the ninth generation International Geomagnetic Reference Field (International Association of Geomagnetism and Aeronomy, 2003). This technique allows us to rapidly calculate a large suite of synthetic anomaly profiles and calculate the root mean square (RMS) error of these synthetics relative to the observed anomaly. Contour plots of RMS error reveal bulls-eyes about the best-fit spreading velocity and intercept age, the width of the bulls-eyes provide a qualitative measure of the error on the best-fit velocities and ages (Fig. 3). We note that this straightforward approach is able to produce synthetic profiles that match the observed anomaly reasonably well; in general the anomalies on the modeled profiles are sharper than those observed. This effect is most likely due to geological complexities such as dipping or diffuse polarity boundaries, varying degrees of magnetization and temporally complicated intrusive relationships within the exposed crust. However our primary aim is to match the sequence and location of magnetic anomalies in order to determine the best-fit half-spreading rate rather than matching the detailed shape of individual anomalies. Although it is possible to improve the fit of the synthetic profiles by varying the dip or magnetization contrast across individual polarity boundaries, doing so is subjective, and has little effect on the best-fit spreading velocities. For example, we have tested the effect of dipping polarity boundaries on the calculated spreading rate along line B–B′ (Figs. 2 and 3d). Allerton and Tivey (2001) suggested that the magnetic polarity boundaries for anomaly C5r.2n dip 20° to the south, so we have modeled this profile using the same parameters as above but with 20° south-dipping polarity boundaries. The resulting anomalies for each chron are less sharp and of slightly lower amplitude than for vertical polarity boundaries. However, the polarity boundaries and hence anomalies are the same distance apart, such that the effect on the best-fit spreading velocities determined using dipping boundaries compared to vertical polarity boundaries is insignificant. For this reason and because the dip of polarity boundaries other than C5r.2n is uncertain, we use vertical magnetic polarity boundaries in our forward models.

5. Results

5.1. Half-spreading rate over Atlantis Bank

Bivariate linear regression of the raw magnetic isochrons and the magnetic polarity of shallow drill cores gives a half-spreading rate of 13.8+1.8/−1.5 km/Myr (95% confidence limits) between chrons C5n and C5Ar (10.4–12.7 Ma; GPTS 2004) (Fig. 2c). The overall ENE-WSW obliquity of the isochrons is not explicitly included in this calculation which calculates an average rate by integrating raw data across Atlantis Bank. Accounting for the average 080° trend of the isochrons by rotating the raw data 10° clockwise, we calculate a spreading rate of 13.2+1.7/−1.3 km/Myr. Although this rate is lower with narrower confidence limits, it is within error of the rate calculated from raw data and it is not clear that the ridge obliquity was constant during the formation of Atlantis Bank. Calculating best-fit spreading rates by forward modeling three anomaly profiles over Atlantis Bank reveals some variation in the best-fit spreading rates (13.5–15.5 km/Myr) implying that the obliquity of the paleo-ridge axis may have changed during the formation of Atlantis Bank (Fig. 3). Thus the validity of making corrections for obliquity is uncertain. As the best-fit spreading rates calculated by forward modeling individual anomaly profiles, by regressing data corrected for the average obliquity and by regressing the raw data are all within error (Fig. 3; Table 1), we will restrict further discussion to spreading rates calculated from the raw data rather than data that has been manipulated to correct for the average obliquity (Table 1).

Regression of all the available Pb/U ages independently corroborates the interpretation of the magnetic data alone and yields a spreading rate of 14.3+15.7/−5.9 km/Myr. Excluding the five anomalously old ages (Schwartz et al., 2005) gives a better constrained half-spreading rate to the south of 14.6+9.3/−3.9 km/Myr. Although the confidence limits on these rates are larger, they agree well with the rate determined from magnetic data alone and these rates are all significantly greater than the 8.6±0.1 km/Myr time-averaged half-spreading rate in this segment since 20 Ma. (Baines et al., 2007).

The Pb/U ages date crystallization of individual magmatic bodies (850±50 °C) (John et al., 2004), which may not be intruded in a regular manner. For example there may be some variation of emplacement both horizontally within the axial valley and with depth below the axial valley. Such variation would, in part, explain the greater uncertainty associated with these spreading rates compared to those determined from the magnetic ages, which provide an average age for cooling of the entire magnetic source layer through the Curie temperature of the gabbros (500–580 °C) (Worm, 2001). Nonetheless, the magnetic ages closely match the Pb/U ages (Fig. 2b) implying rapid cooling from 850± 50 °C to below 500 °C in ≪0.4 Ma (John et al., 2004; Schwartz et al., 2005), a result consistent with rapid cooling rates calculated from Ca-in-olivine diffusion profiles for rocks in Hole 735B (Coogan et al., 2007). As cooling rates were so rapid, the magnetic ages and U/Pb ages are equivalent within error and have been used together to calculate a half-spreading rate for the Antarctic plate of 14.1+1.8/−1.5 km/Myr during detachment faulting (10.3–12.7 Ma) (Table 1; Fig. 2).

Sensu-strictu, the ~14 km/Myr rate over Atlantis Bank does not record the slip rate along the detachment fault, but rather the apparent rate of plate spreading. Ridge-parallel normal faults observed in bathymetric data cutting the detachment fault suggest a

Please cite this article as: Baines, A.G., et al., The rate of oceanic detachment faulting at Atlantis Bank, SW Indian Ridge Earth and Planetary Science Letters (2008), doi:10.1016/j.epsl.2008.06.013

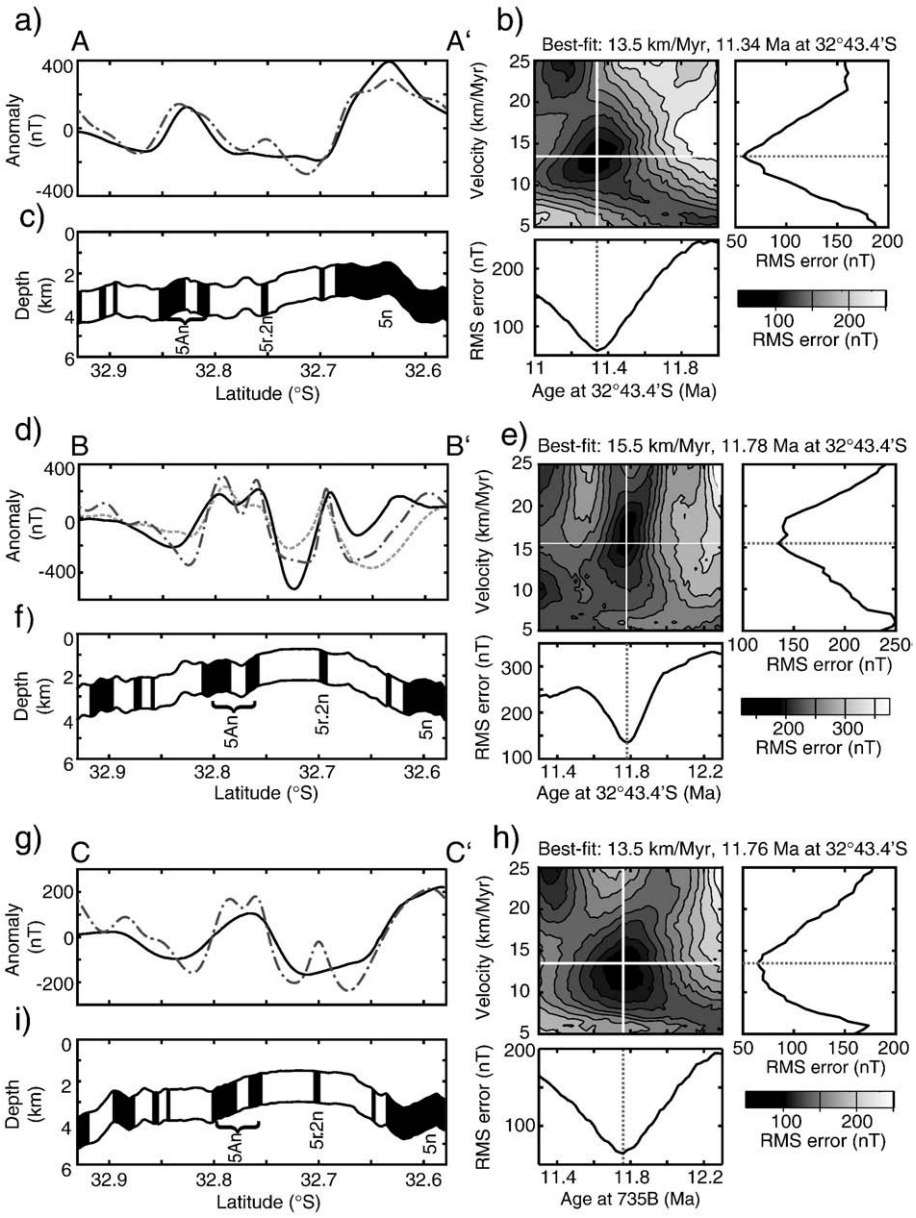

Fig. 3. Results of forward models for the three profiles: lines A–A′ (a–c), B–B′ (d–f) and C–C′ (g–i) shown in Fig. 2. a), d) and g) Observed magnetic anomaly profiles (solid black lines) and synthetic magnetic anomaly profiles assuming vertical polarity boundaries (dashed-dot dark grey lines), d) also shows a forward model calculated in GM-SYS assuming identical parameters but for polarity boundaries that dip 20° to the south (pale dashed line). b), e) and h) root mean square (rms) misfit between models and observations. Contour plots of rms misfit for models run with different spreading velocity and intercept age at 32°43.4′S, white lines show the locations of profiles through the minima plotted below and to the right of the contour plots. c), f) and i) the magnetic polarity structure as defined for the best-fit spreading rate and intercept age using the geomagnetic polarity timescale 2004 and the observed bathymetry for a 1.5-km-thick source layer. Black boxes — normal polarity (+2 A/m), white — reversed polarity (−2 A/m).

component of later extension that would lead to an overestimated rate of detachment faulting (Fig. 1). However the throw on these faults is relatively minor, scarps are <600 m high, such that the total magnitude of extension on these faults is likely to be <1.5 km. Accounting for this late-stage extension would reduce the half-spreading rate we have determined by <0.7 km/Myr, which is less than the calculated error on half-spreading rate. Therefore the ~14 km/Myr rate inferred over Atlantis Bank likely approximates the time-averaged slip rate on the detachment fault system.

5.2. Regional analysis

A regional analysis of spreading rates from the SWIR surrounding Atlantis Bank since 26 Ma, was presented by Baines et al. (2007). Of particular relevance here, they analysed data over a period from 10.4–15.6 Ma (C5n to C5Br) that includes the formation of Atlantis Bank and showed that regionally the full-spreading rate increased to an average of 15.7±0.7 km/Myr. They also showed that although the segment containing Atlantis Bank (segment AN-1) was spreading asymmetrically, the segment to the east (segment AN-2), was spreading symmetrically over the same period. This difference in spreading asymmetry led to relative migration of the spreading ridges in each segment and a reduction in the offset of the intervening non-transform discontinuity (Fig. 4b). We note that this reduction was most rapid at the time Atlantis Bank formed and that the half-spreading rate determined over Atlantis Bank from 10.4–12.7 Ma is significantly faster than the average of 10.4±0.6 km/Myr over the longer period from 10.4–15.6 Ma (Baines et al., 2007). Before 12.7 Ma, we calculate a half-spreading rate of 7.3+1.6/−1.5 km/Myr (12.7–15.6 Ma) while after 10.4 Ma the half-spreading rate was 8.9±0.7 km/

Please cite this article as: Baines, A.G., et al., The rate of oceanic detachment faulting at Atlantis Bank, SW Indian Ridge Earth and Planetary Science Letters (2008), doi:10.1016/j.epsl.2008.06.013

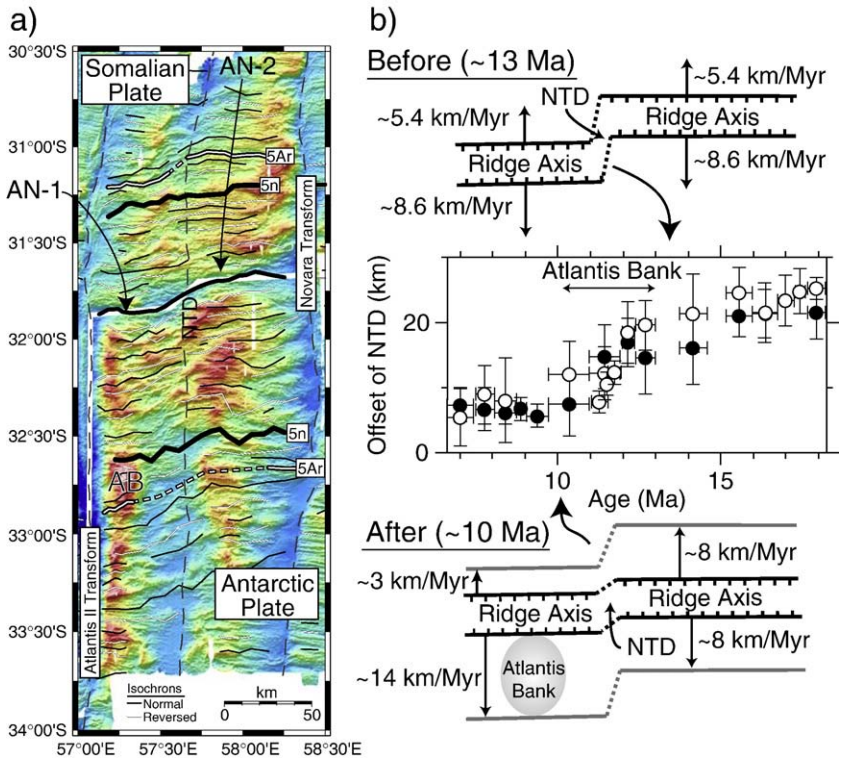

Fig. 4. Regional analysis of spreading during the formation of Atlantis Bank. a) Magnetic isochrons for the zone between the Atlantis II and Novara Transform faults after Baines et al. (2007). Current plate-boundary — thick grey line, normal polarity isochrons — black lines, reverse polarity isochrons — grey lines, fracture zones — Dashed light grey lines, AB — Atlantis Bank, NTD — 56°40′E non-transform discontinuity. Bathymetry shown with same palette as in Fig. 2b) without the false illumination. b) Closure of the 57°40′E non-transform discontinuity and ridge migration. A graph of the spreading-parallel offset of magnetic isochrons across the 57°40′E non-transform discontinuity versus age both north (filled circles) and south (open circles) of the ridge axis (modified from Baines et al., 2007). The offset across the non-transform discontinuity reduced rapidly during the formation of Atlantis Bank. Cartoons above and below the graph show the ridge geometry and approximate spreading rates before detachment faulting (~13 Ma) and at the cessation of detachment faulting (~10 Ma) respectively.

Myr (4.7–10.4 Ma; Baines et al., 2007). These rates are both significantly slower than the half-spreading rate calculated over Atlantis Bank (14.1+1.8/−1.5 km/Myr), so suggest that the regional increase in full-spreading rate, asymmetric spreading and shortening of the non-transform discontinuity may all be associated with changes in plate kinematics that coincide with the formation of Atlantis Bank.

To further investigate this potentially anomalous period from 10.4–12.7 Ma, we use the regional magnetic anomaly data to further constrain the kinematics of sea-floor spreading during the formation of Atlantis Bank. However, away from the anomalously elevated Atlantis Bank, greater attenuation of the magnetic signal from the deeper source layer reduces the resolution of sea-surface magnetic data. The slower average half-spreading rate to the north of segments AN-1 and AN-2 (5.4 km/Myr) also compresses the sequence of anomalies with the result that many of the shorter duration magnetic polarity chrons observed at Atlantis Bank cannot be resolved, and only isochrons of long duration (>400 kyr) can be identified. Despite the lower resolution of these data, anomalies C5n, C5r, C5An and C5Ar have been identified on the Somalian Plate conjugate to Atlantis Bank (segment AN-1; Hosford et al., 2003; Baines et al., 2007) and on both plates in the spreading segment immediately to the east (segment AN-2; Hosford et al., 2003; Baines et al., 2007; Fig. 4a). These isochrons are used to calculate spreading rates using the same bivariate regression methodology used over Atlantis Bank (Table 2). Full-spreading rates calculated directly using the total distance between isochrons north and south of the axis are 17.2+2.8/−1.4 km/Myr and 16.4+1.3/−1.4 km/Myr for segments AN-1 and AN-2 respectively. These spreading rates are within error of each other, so suggest a regionally elevated full-spreading rate during the formation of Atlantis Bank, which was significantly faster than the 14 km/Myr average full-spreading rate since 20 Ma. Although the calculated rates from 10.4–12.7 Ma are not significantly greater than the average 15.7±0.7 km/Myr rate calculated over the longer period from 10.4–15.6 Ma, they hint that regionally elevated full-spreading rates could be restricted to the time that Atlantis Bank formed.

The elevated full-spreading rate of ~17 km/Myr taken together with the 14.1 km/Myr half-spreading rate over Atlantis Bank suggests a half-spreading rate for the Somalian Plate in segment AN-1 of ~3 km/Myr, although direct calculation using the isochrons on the Somalian Plate suggests a half-spreading rate of 4.6+1.3/−1.6 km/Myr. The apparent discrepancy between these half-spreading rates reflects errors associated with determining a half-spreading rate from the closely spaced and poorly defined anomalies north of the spreading axis. However, it is clear from these data that spreading in segment AN-1 was highly asymmetric, with 80±15% of the full-spreading rate accommodated to the south by slip on the detachment fault.

Table 2
Regional spreading rates from 10.4–12.7 Ma (C5n–C5Ar) calculated from magnetic anomaly data

Segment	Description	Rate (km/Myr)	95% Confidence Limits	
			Plus	Minus
AN-1	Full-spreading rate	17.2	2.8	1.4
	Antarctic Plate (Atlantis Bank)	13.8	1.8	1.5
	Somalian Plate	4.6	1.3	1.6
AN-2	Full-spreading rate	16.4	1.3	1.4
	Antarctic Plate	8.3	0.7	0.7
	Somalian Plate	8.3	0.9	1.1

Please cite this article as: Baines, A.G., et al., The rate of oceanic detachment faulting at Atlantis Bank, SW Indian Ridge Earth and Planetary Science Letters (2008), doi:10.1016/j.epsl.2008.06.013

In contrast for segment AN-2 over the same period spreading rates were symmetric with half-spreading rates of 8.3+0.9/−1.1 km/Myr for the Somalian Plate and 8.3+0.7/−0.7 km/Myr for the Antarctic Plate. This means that ridge segments AN-1 and AN-2 migrated relative to one another in a dextral sense at ~4–7 km/Myr, reducing the spreading-parallel offset across the non-transform discontinuity that separates these segments (Fig. 4b). This reduction may also be related to shallowing of the bathymetric trace of this offset at this time (Fig. 4a) (Hosford et al., 2003; Baines et al., 2007). We stress that extremely asymmetric spreading was confined to segment AN-1 and to the formation of Atlantis Bank, so may be directly associated with detachment faulting.

6. Discussion

Many plate-kinematic observations suggest that Atlantis Bank did not form during a period of "normal" symmetric spreading. In particular, asymmetric spreading rates have dominated the region about the Atlantis II Transform fault since at least 20 Ma (Dick et al., 1991; Hosford et al., 2003) and resulted in major changes in plate-boundary geometry including significant growth of the adjacent Atlantis II Transform fault (Baines et al., 2007). Furthermore, a rotation in plate-spreading direction ~20 Ma resulted in 12 Myr of transtension on the Atlantis II Transform fault (Dick et al., 1991; Baines et al., 2007). The formation of Atlantis Bank itself was associated with particularly extreme asymmetric spreading and a short-lived regional increase in the full-spreading rate. Here we discuss the role each of these factors may have played in the initiation of detachment faulting.

Atlantis Bank is the only oceanic core-complex observed in Segment AN-1, yet spreading in this segment has been asymmetric since 20 Ma and the Atlantis II Transform was in transtension from ~20 to 8 Ma. Thus neither transtension nor asymmetric spreading associated with the plate-boundary's long term evolution can fully explain the single, relatively short-lived episode of detachment faulting in this area. Using similar logic, we note that the short-lived regional increase in the full-spreading rate, which coincides with the formation of Atlantis Bank, is not associated with a spate of core-complex formation regionally along the SWIR (e.g. Baines et al., 2007; Cannat et al., 2006). So this pulse of faster spreading is unlikely to be the sole cause of detachment faulting. We suggest that the formation of Atlantis Bank may reflect a combination of these factors, such that the location of Atlantis Bank in segment AN-1 was controlled by anomalous stress conditions at the ridge-transform intersection associated with transtension along and growth of the weak Atlantis II Transform fault (Baines et al., 2003, 2007), while the initiation of detachment faulting coincides with the regional increase in full-spreading rate ~13 Ma.

Several authors have noted the reorientation and concentration of regional tectonic stresses at ridge-transform intersections (e.g. Fujita and Sleep, 1978; Phipps Morgan and Parmentier, 1984; Furlong et al., 2001; van Wilk and Blackman, 2005) and some have suggested that these effects may promote the formation of oceanic core-complexes (Furlong et al., 2001). Transtension on the Atlantis II Transform fault may have amplified these effects, such that a zone of high stress extended further from the transform fault into the inside corner of the ridge-transform intersection (Fujita and Sleep, 1978). Furthermore, long-lived fast-to-the-south asymmetric spreading in segment AN-1 likely thermally weakened the inside corner (Sleep, 1975; Fujita and Sleep, 1978). These factors suggest that the inside corner of segment AN-1 was relatively weak, under elevated stress and so was predisposed to detachment faulting. However, in isolation, these factors may have been insufficient to trigger detachment faulting and further perturbation to the system was necessary; in this case the increase in full-spreading rate 12.7–10.4 Ma. This increase in spreading rate may have acted to trigger detachment faulting in a number of ways; for example by altering the regional tectonic stress conditions, mantle flow dynamics or relative proportion of extension accommodated magmatically. The complex interaction of kinematic factors and their likely role in the initiation of detachment fault at Atlantis Bank contrasts with other regions on the mid-ocean ridge system where detachment faulting is more common and may be the dominant mode of sea-floor spreading (Smith et al., 2006, 2008). In these settings the full-spreading rate and/or magma supply may be better suited for detachment faulting (e.g. Buck et al., 2005; Tucholke et al., 2008) than the eastern SWIR where detachment faults occur less frequently (Cannat et al., 2006; Baines et al., 2007).

Although the sense of asymmetric spreading during detachment faulting at Atlantis Bank is consistent with the long term evolution of the SWIR and growth of the Atlantis II Transform fault (Baines et al., 2007), the magnitude of asymmetry is extreme and constrained to Atlantis Bank alone. We suggest that the extremely asymmetric half-spreading rates are linked to the asymmetric process of oceanic detachment faulting itself, such that strain localization on the detachment fault reduced extensional stresses within the axial valley and limited magmatic extension by diking, increasing the proportion of plate-motion accommodated by the fault and leading to highly asymmetric spreading rates (Fig. 5). Thus, oceanic detachment

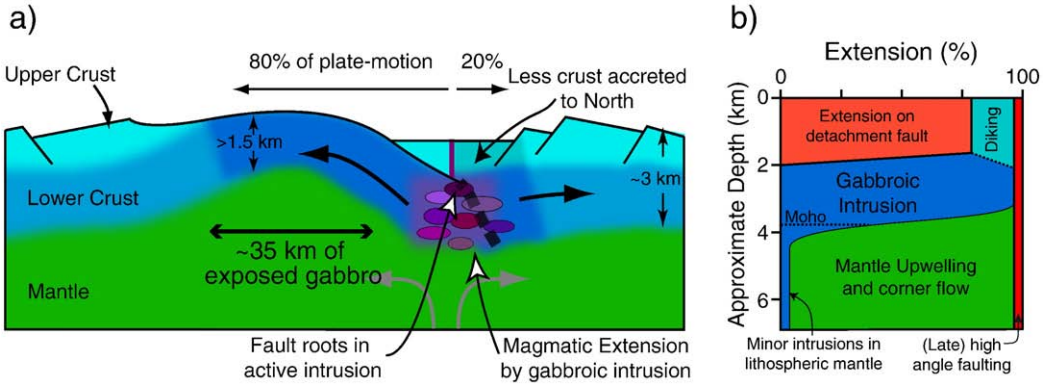

Fig. 5. a) Cartoon of asymmetric spreading and the distribution of crustal accretion during detachment faulting at Atlantis Bank. Darker shaded crust was accreted during active detachment faulting. The majority of material accreted beneath, and was denuded by, the detachment fault. b) Schematic model of how extensional strain was accommodated with depth during detachment faulting. In the upper crust the majority of extension was accommodated by the detachment fault, while dyking in the axial valley was likely to accommodate much of the remaining extension. The detachment fault likely rooted in a zone of magmatic accretion at 1.5–2 km depth (Vanko and Stakes, 1991) and is represented by a gradational transition from dominantly tectonic extension to magmatic accretion at this level. In the middle–lower crust, extension was dominated by magmatic extension during the intrusion of gabbroic rocks, the majority of which were then uplifted and exposed by the detachment fault. Below the oceanic crust (>3 km: Muller et al., 1997), extension was probably accommodated by upwelling mantle and by minor gabbroic intrusion into the lithospheric mantle (Lizarralde et al., 2004; Schwartz et al., 2005). We include a component of extension that was likely accommodated by high-angle normal faults that penetrate the lithospheric mantle to >6 km (Huang and Solomon, 1988).

Please cite this article as: Baines, A.G., et al., The rate of oceanic detachment faulting at Atlantis Bank, SW Indian Ridge Earth and Planetary Science Letters (2008), doi:10.1016/j.epsl.2008.06.013

faulting may commonly produce asymmetric plate-spreading rates. This inference is supported by less well-constrained data from other oceanic core-complexes. Specifically, we note that asymmetric spreading rates have been inferred at FUJI dome (10.8 km/Myr, 77% of spreading) (Searle et al., 2003), the Kane megamullion (17.9 km/Myr, 63% of spreading) (Schulz et al., 1988), Atlantis Massif (>16 km/Myr, >70% of spreading) (Grimes et al., in press) and for detachment faults at the Australian–Antarctic Discordance (up to 75% of spreading) (Okino et al., 2004). Another implication, if asymmetric spreading rates are an inherent feature of detachment faulting is that oceanic detachment faulting will necessarily lead to relative ridge migration and changes in the plate-boundary geometry, similar to those observed at Atlantis Bank (Fig. 4).

Although in the above discussion we have primarily considered kinematic triggers for detachment faulting, several authors have taken the exhumation of peridotites to infer limited magmatism in the footwall of oceanic detachment faults, and suggested that the formation of oceanic core-complexes is linked to variations in the supply of melt to the ridge axis (Tucholke et al., 1998; Buck et al., 2005). However, significant thicknesses of gabbros recovered from several oceanic core-complexes including Atlantis Bank suggest that magmatic intrusion may continue in the footwall of active detachment faults (Natland and Dick, 2002; Ildefonse et al., 2007; Dick et al., 2008). Furthermore Dick et al. (2008) have documented spreading-perpendicular variations in footwall lithology at the Kane megamullion where between two gabbroic plutons displaying high-temperature crystal plastic deformation (similar to Atlantis Bank) a section of dominantly mantle rocks has been recovered. Our observations of systematic younging of magnetic and Pb/U zircon ages towards the ridge axis at Atlantis Bank also emphasize that gabbroic accretion continued during >2 Myr of detachment faulting and supports the interpretation that magma supply to segment AN-1 has not changed significantly since 14 Ma (Coogan et al., 2004). However, although magma supply to segment AN-1 may have been unchanged, the increased full-spreading rate during the formation of Atlantis Bank may alter the relative proportion of extension accommodated magmatically and so act to promote detachment faulting (Tucholke et al., 2008).

In the same way that magma supply varies between oceanic core-complexes so do the accommodation of deformation and observed tectonic rotations. At some oceanic core-complexes on the Mid-Atlantic Ridge where gabbro has been recovered, tectonic rotation below the Curie temperature may have been 50–80° (Garcés and Gee, 2007) and deformation appears to have localized in serpentinized fault zones surrounding large, undeformed, primitive gabbro bodies that also accreted during detachment faulting (Grimes et al., in press) but at greater depth (~6 km) and were largely solid during denudation (Ildefonse et al., 2007). In contrast, at Atlantis Bank gabbros accreted at 1.5–2 km depth (Vanko and Stakes, 1991) are crystal plastically deformed and underwent ~20° rotation below the Curie temperature. Although it is not possible to constrain tectonic rotation above the Curie temperature, at Atlantis Bank, the good agreement between Pb/U zircon ages and magnetic ages (John et al., 2004; Schwartz et al., 2005), fast cooling rates calculated from geospeedometry (Coogan et al., 2007) and the apparently rapid acquisition of magnetization (Pariso and Johnson, 1993; Worm, 2001) highlight that cooling to below Curie temperature after gabbroic accretion was likely rapid, such that significant tectonic rotations before the gabbros cooled below the Curie temperature are unlikely. However, large tectonic rotation above the Curie temperature may not be necessary as we can reconcile the low tectonic rotation observed in these shallowly intruded gabbros with the model of denudation along detachment faults that steepen with depth (Buck, 1988; deMartin et al., 2007). In such a model, shallowly intruded gabbros will undergo less tectonic rotation than those denuded from greater depth. Thus Atlantis Bank may represent a magmatically robust “hot” shallow end-member to the spectrum of conditions and magma supply that form oceanic detachment faults.

In contrast to the observed variations in magma supply, localization of deformation and tectonic rotation between oceanic core-complexes, we have noted that asymmetric spreading rates during detachment faulting appear common. We therefore present a kinematically constrained model for the accommodation of extension with depth during the formation of Atlantis Bank (Fig. 5); we suggest that the detachment fault rooted at the dyke–gabbro transition in a zone of active magmatic accretion (Dick et al., 2000). Below this, the majority of extension was accommodated magmatically such that the plate-boundary in the lower–middle crust was represented by a zone of gabbroic accretion (Fig. 5). Given the asymmetric kinematics of plate-motion, the majority (~80%) of gabbro that accreted in this zone was likely denuded by the detachment fault, so is now exposed on the Antarctic Plate at Atlantis Bank. Thus lower crustal accretion may have continued unabated during detachment faulting, while in the upper crust tectonic extension on the detachment fault was dominant and magmatic extension was relatively reduced, a model that is consistent with observations of reduced magmatism in the upper crust during continental detachment faulting (Gans and Bohrson, 1998). Below the zone of magmatic accretion in the middle–lower crust, extension would be primarily accommodated by ductile deformation and upwelling of mantle, either by pervasive flow or localized deformation on discrete shear zones (Jaroslow et al., 1996; Warren and Hirth, 2006; Achenbach et al., 2007). Magmatic accretion in the mantle lithosphere may have also accommodated a component of extension (Lizarralde et al., 2004; Schwartz et al., 2005).

7. Conclusions

At Atlantis Bank we calculate a time-averaged rate of detachment faulting of 14.1 + 1.8/− 1.5 km/Myr using both magnetic anomaly data and SHRIMP Pb/U zircon ages. At this time, the full-spreading rate of the SWIR increased from the average of 14 km/Myr to ~17 km/Myr for ~2.3 Myr, so implies highly asymmetric spreading with ~80% of plate-motion accommodated by detachment faulting. Therefore, the detachment fault system acted as the primary plate-boundary in the upper crust. Asymmetric spreading was confined to the ridge segment containing Atlantis Bank resulting in this segment's northward migration relative to its symmetric spreading eastern neighbour and the consequent shortening of the intervening non-transform discontinuity.

A regional analysis suggests that the initiation of oceanic detachment faulting at Atlantis Bank may have been influenced by a combination of kinematic factors; specifically a short-lived regional increase in full-spreading rate, the long-lived evolution of plate-boundary geometry and Atlantis Bank's proximity to the growing and weak Atlantis II Transform fault (Baines et al., 2007), which was undergoing transtension following a rotation in plate-spreading direction ~20 Ma (Baines et al., 2003; Dick et al., 1991).

The Pb/U ages further highlight that magmatic accretion and faulting were intimately related at Atlantis Bank and occurred simultaneously for >2 Myr creating and exposing a >1.5-km-thick layer of gabbro for over 35 km parallel-to-spreading. We propose a model of sea-floor spreading during detachment faulting at Atlantis Bank where the majority of extension in the upper crust was accommodated by detachment faulting with relatively reduced extension by magmatic diking in the upper crust. The detachment fault rooted in a zone of magmatic accretion in the lower–middle crust below which extension was primarily accommodated by magmatic intrusion, or ductile deformation and upwelling of mantle.

Although Atlantis Bank's tectonic setting may have played a role in triggering this oceanic detachment fault, the highly asymmetric spreading rates were restricted to Atlantis Bank and asymmetric half-spreading rates have been observed at several other oceanic core-

Please cite this article as: Baines, A.G., et al., The rate of oceanic detachment faulting at Atlantis Bank, SW Indian Ridge Earth and Planetary Science Letters (2008), doi:10.1016/j.epsl.2008.06.013

complexes (Schulz et al., 1988; Searle et al., 2003; Okino et al., 2004; Grimes et al., in press). Therefore we suggest that highly asymmetric spreading rates may be a characteristic feature of oceanic detachment faulting.

Acknowledgements

This manuscript benefited greatly from discussions with and the insightful comments of H. Dick, C. Grimes and E. Miranda. Comments on an early version of the manuscript by L. Coogan helped improve and clarify our arguments, while comments from two anonymous reviewers further improved the manuscript. Funding for this work came from a JOI-Schlanger Fellowship to Baines, NSF grant # 0352054 to Cheadle and John, and W.C. Hayes Fellowship and NASA Space Grant to Schwartz. Figs. 2 and 4 were created using the Generic Mapping Tools (GMT) software (Wessel and Smith, 1998).

References

Achenbach, K.L., Cheadle, M.J., Dick, H.J.B., Swapp, S., 2007. Deformation and melt–rock interaction in peridotites from the Atlantis II transform, SWIR: evidence for diffuse melt percolation in deep lithospheric mantle. EOS Trans. AGU 88 (52) (Fall Meet. Suppl., Abstract T52B-04).

Allerton, S., Tivey, M.A., 2001. Magnetic polarity structure of the lower oceanic crust. Geophys. Res. Lett. 28 (3), 423–426.

Allerton, S., Escartin, J., Searle, R.C., 2000. Extremely asymmetric magmatic accretion of oceanic crust at the ends of slow-spreading ridge segments. Geology 28 (2), 179–182.

Baines, A.G., Cheadle, M.J., Dick, H.J.B., Hosford Scheirer, A., John, B.E., Kusznir, N.J., Matsumoto, T., 2003. A mechanism for generating the anomalous uplift of oceanic core-complexes: Atlantis Bank, SW Indian Ridge. Geology 31 (12), 1105–1108.

Baines, A.G., Cheadle, M.J., Dick, H.J.B., Hosford Scheirer, A., John, B.E., Kusznir, N.J., Matsumoto, T., 2007. The evolution of the Southwest Indian Ridge from 55°45′E–62°E: changes in plate-boundary geometry since 26 Ma. Geochem. Geophys. Geosyst. 8, Q06022. doi:10.1029/2006GC001559.

Blackman, D.K., Cann, J.R., Janssen, B., Smith, D.K., 1998. Origin of extensional core complexes: evidence from the Mid-Atlantic Ridge at Atlantis Fracture Zone. J. Geophys. Res. 103 (B9), 21315–21333.

Buck, W.R., 1988. Flexural rotation of normal faults. Tectonics 7 (5), 959–973.

Buck, W.R., Lavier, L.L., Poliakov, A.N.B., 2005. Modes of faulting at mid-ocean ridges. Nature 434, 719–723.

Cannat, M., Sauter, D., Mendel, V., Ruellan, E., Okino, K., Escartin, J., Combier, V., Baala, M., 2006. Modes of seafloor generation at a melt-poor ultraslow-spreading ridge. Geology 34 (7), 605–608. doi:10.1130/G22486.

Cann, J.R., Blackman, D.K., Smith, D.K., McAllister, E., Janssen, B., Mello, S., Avgerinos, E., Pascos, A.R., Escartin, J., 1997. Corrugated slip surfaces formed at ridge-transform intersections on the Mid-Atlantic Ridge. Nature 385, 329–332.

Coogan, L.A., Thompson, G.M., MacLeod, C.J., Dick, H.J.B., Edwards, S.J., Hosford Scheirer, A., Barry, T.L., 2004. A combined basalt and peridotite perspective on 14 million years of melt generation at the Atlantis Bank segment of the Southwest Indian Ridge; evidence for temporal changes in mantle dynamics. Chem. Geol. 207 (1–2), 13–30.

Coogan, L.A., Jenkin, G.R.T., Wilson, R.N., 2007. Contrasting cooling rates in the lower oceanic crust at fast- and slow-spreading ridges revealed by Geospeedometry. J. Petrol. 48, 2211–2231.

deMartin, B.J., Reves-Sohn, R.A., Canales, J.P., Humphris, S.E., 2007. Kinematics and geometry of active detachment faulting beneath the Trans-Atlantic Geotraverse (TAG)hydrothermal field on the Mid-Atlantic Ridge. Geology 35 (8), 711–714.

Dick, H.J.B., Schouten, H., Meyer, P.S., Gallo, D.G., Bergh, H., Tyce, R., Patriat, P., Johnson, K.T.M., Snow, J., Fisher, A., 1991. Tectonic evolution of the Atlantis II fracture zone. In: Von Herzen, R.P., Fox, J., Palmer-Julson, A., Robinson, P.R. (Eds.), Proceedings of the Ocean Drilling Program, Scientific Result, vol. 118. Ocean Drilling Program, College Station, TX, pp. 359–398.

Dick, H.J.B., Natland, J.H., Alt, J.C., Bach, W., Bideau, D., Gee, J.S., Haggas, S., Hertogen, J.G.H., Hirth, G., Holm, P.M., Ildefonse, B., Iturrino, G.J., John, B.E., Kelley, D.S., Kikawa, E., Kingdon, A., LeRoux, P.J., Maeda, J., Meyer, P.S., Miller, D.J., Naslund, H.R., Niu, Y.-L., Robinson, P.T., Snow, J., Stephen, R.A., Trimby, P.W., Worm, H.-U., Yoshinobu, A., 2000. A long in situ section of the lower ocean crust: results of ODP Leg 176 drilling at the Southwest Indian Ridge. Earth Planet. Sci. Lett. 179, 31–51.

Dick, H.J.B., Tivey, M.A., Tucholke, B.E., 2008. Plutonic foundation of a slow-spreading ridge segment: the oceanic complex at kane megamullion, 23°30′N, 45°20′W. Geochem. Geophys. Geosyst. 9 (9), Q05014.

Efron, B., Tibshirani, R.J., 1994. An Introduction to the Bootstrap Method. CRC Press, Boca Raton, Fl.

Escartin, J., Mével, C., MacLeod, C.J., McCaig, A.M., 2003. Constraints on deformation conditions and the origin of oceanic detachments: the Mid-Atlantic core complex at 15°45′N. Geochem. Geophys. Geosyst. 4 (8), 1067. doi:10.1029/2002GC000472.

Fujita, K., Sleep, N.H., 1978. Membrane stresses near mid-ocean ridge-transform intersections. Tectonophysics 50, 207–221.

Furlong, K.P., Sheaffer, S.D., Malservisi, R., 2001. Thermal–rheological controls on deformation within oceanic transforms. In: Holdsworth, R.E., Strachan, R.A., Maglaughlin, J.F., Knipe, R.J. (Eds.), Geological Society Special Publication,186: The Nature and Tectonic Significance of Fault-Zone Weakening, pp. 65–83.

Gans, P.B., Bohrson, W.A., 1998. Suppression of volcanism during rapid extension in the Basin and Range Province, United States. Science 279, 66–68.

Garcés, M., Gee, J.S., 2007. Paleomagnetic evidence of large footwall rotations associated with low-angle faults at the Mid-Atlantic Ridge. Geology 35 (3), 279–282.

Grimes, C.B., John, B.E., Cheadle, M.J., Wooden, J.L., in press. Protracted construction of gabbroic crust at a slow-spreading ridge: Constraints from 206Pb/238U zircon ages from Atlantis Massif and IODP Hole U1309D (30°N MAR). Geochem. Geophys. Geosyst. doi:10.1029/2008GC002063.

Horner-Johnson, B.C., Gordon, R.G., Cowles, S.M., Argus, D.F., 2005. The angular velocity of Nubia relative to Somalia and the location of the Nubia–Somalia–Antarctica triple junction. Geophysical Journal International 162, 221–238.

Hosford, A., Tivey, M.A., Matsumoto, T., Dick, H.J.B., Schouten, H., Kinoshita, H., 2003. Crustal magnetization and accretion at the Southwest Indian Ridge near the Atlantis II fracture zone, 0–25 Ma. J. Geophys. Res. 108 (B3), 2169. doi:10.1029/2001JB000604.

Huang, P.Y., Solomon, S.C., 1988. Centroid depths of mid-ocean ridge earthquakes: dependence on spreading rate. J. Geophys. Res. 93 (B11), 13445–13477.

Ildefonse, B., Blackman, D.K., John, B.E., Ohara, Y., Miller, D.J., MacLeod, C.J., Party, I.O.D.P.E.S., 2007. Oceanic core complexes and crustal accretion at slow-spreading ridges. Geology 35 (7), 623–626.

Jaroslow, G.E., Hirth, G., Dick, H.J.B., 1996. Abyssal peridotite mylonites: implications for grain-size sensitive flow and strain localization in the oceanic lithosphere. Tectonophysics 256, 17–37.

John, B.E., Foster, D.A., Murphy, J.M., Cheadle, M.J., Baines, A.G., Fanning, C.M., Copeland, P., 2004. Determining the cooling history of in situ lower oceanic crust — Atlantis Bank SW Indian Ridge. Earth Planet. Sci. Lett. 222 (1), 145–160.

Kikawa, E., Pariso, J.E., 1991. Magnetic Properties of Gabbros from Hole 735B, Southwest Indian Ridge. In: Von Herzen, R.P., Fox, J., Palmer-Julson, A., Robinson, P.R. (Eds.), Proceedings of the Ocean Drilling Program, Scientific Results, vol. 118. Ocean Drilling Program, College Station, TX, pp. 285–307.

Lizarralde, D., Gaherty, J.B., Collins, J.A., Hirth, G., Kim, S.D., 2004. Spreading-rate dependence of melt extraction at mid-ocean ridges from mantle seismic refraction data. Nature 432, 744–747.

Matsumoto, T., Dick, H.J.B., Party, A.S., 2002. Investigation of Atlantis Bank and the SW Indian Ridge from 56°E to 58°E: preliminary report. JAMSTEC Deep Sea Research, Yokosuka, Japan, p. 463.

Miranda, E.A., Structural Development of the Atlantis Bank Oceanic Detachment Fault System, Southwest Indian Ridge, PhD thesis, University of Wyoming, Laramie, WY, 2006.

Muller, M.R., Robinson, C.J., Minshull, T.A., White, R.S., Bickle, M.J., 1997. Thin crust beneath ocean drilling program borehole 735B at the Southwest Indian Ridge? Earth Planet. Sci. Lett. 148, 93–107.

Natland, J.H., Dick, H.J.B., 2002. Stratigraphy and composition of gabbros drilled in Ocean Drilling Program Hole 735B, Southwest Indian Ridge; a synthesis of geochemical data. Proceedings of the Ocean Drilling Program, Scientific Results, vol. 179, p. 69.

Ogg, J.G., Smith, A.G., 2004. The geomagnetic polarity time scale. In: Gradstein, F.M., Ogg, J.G., Smith, A.G. (Eds.), A Geological Time Scale 2004. Cambridge University Press, Cambridge, pp. 63–86.

Okino, K., Matsuda, K., Christie, D.M., Nogi, Y., Koizumi, K.-I., 2004. Development of oceanic detachment and asymmetric spreading at the Australian–Antarctic Discordance. Geochem. Geophys. Geosyst. 5 (12), Q12012. doi:10.1029/2004GC000793.

Pariso, J.E., Johnson, H.P., 1993. Do layer 3 rocks make a significant contribution to marine magnetic anomalies? In situ magnetization of gabbro at Ocean Drilling Program Hole 735B. J. Geophys. Res. 98 (B9), 16033–16052.

Parker, R.L., 1972. The rapid calculation of potential anomalies. Geophys. J. R. Astron. Soc. 31, 447–455.

Phipps Morgan, J., Parmentier, E.M., 1984. Lithospheric stress near a ridge-transform intersection. Geophys. Res. Lett. 11, 113–116.

Schulz, N.J., Detrick, R.S., Miller, S.P., 1988. Two- and three-dimensional inversions of magnetic anomalies in the MARK Area (Mid-Atlantic Ridge 23° N). Mar. Geophys. Res. 10, 41–57.

Schwartz, J.J., John, B.E., Cheadle, M.J., Miranda, E.A., Grimes, C.B., Wooden, J.L., Dick, H.J.B., 2005. Dating growth of oceanic crust at a slow-spreading ridge. Science 310, 654–657.

Searle, R.C., Cannat, M., Fujioka, K., Mével, C., Fujimoto, H., Bralee, A., Parson, L., 2003. FUJI Dome: a large detachment fault near 64°E on the very slow-spreading southwest Indian Ridge. Geochem. Geophys. Geosyst. 4 (8), 25. doi:10.1029/2003GC000519.

Shipboard Scientific Party, 1999. Site 735B. In: Dick, H.J.B., Natland, J.H., Miller, D.J. (Eds.), Proceedings ODP, Initial Reports 176. Ocean Drilling Program, College Station, TX, pp. 1–314.

Sleep, N.H., 1975. Formation of oceanic crust: some thermal constraints. J. Geophys. Res. 89 (29), 4037–4042.

Smith, D.K., Cann, J.R., Escartin, J., 2006. Widespread active detachment faulting and core complex formation near 13°N on the Mid-Atlantic Ridge. Nature 442, 440–443.

Smith, D.K., J. Escartin, H. Schouten, J.R. Cann, 2008. Fault rotation and core complex formation: significant processes in seafloor formation at slow-spreading mid-ocean ridges (Mid-Atlantic Ridge, 13°–15°N). Geochem. Geophys. Geosyst. 9 (3), Q03003. doi:10.1029/2007GC001699.

Tucholke, B.E., Lin, J., Kleinrock, M.C., 1998. Megamullions and mullion structure defining oceanic metamorphic core complexes on the Mid-Atlantic Ridge. J. Geophys. Res. 103 (B5), 9857–9866.

Please cite this article as: Baines, A.G., et al., The rate of oceanic detachment faulting at Atlantis Bank, SW Indian Ridge Earth and Planetary Science Letters (2008), doi:10.1016/j.epsl.2008.06.013

Tucholke, B.E., Fujioka, K., Ishihara, T., Hirth, G., Kinoshita, M., 2001. Submersible study of an oceanic megamullion in the central North Atlantic. J. Geophys. Res. 106 (B8), 16145–16161.

Tucholke, B.E., Behn, M.D., Buck, W.R., Lin, J., 2008. Role of melt supply in oceanic detachment faulting and formation of megamullions. Geology 36 (6), 455–458. doi:10.1130/G24639A.

Vanko, D.A., Stakes, D.S., 1991. Fluids in oceanic Layer 3: evidence from veined rocks, Hole 735B, Southwest Indian Ridge. Proceedings of the Ocean Drilling Program, Scientific Results, vol. 118, pp. 181–215.

van Wilk, J.W., Blackman, D.K., 2005. Deformation of oceanic lithosphere near slow-spreading ridge discontinuities. Tectonophysics 407, 211–225.

Warren, J.M., Hirth, G., 2006. Grain size sensitive deformation mechanisms in naturally deformed peridotites. Earth Planet. Sci. Lett. 248, 438–450.

Wessel, P., Smith, W.H.F., 1998. New improved version of Generic Mapping Tools released. EOS, Trans. AGU 79 (47), 579.

Worm, H.-U., 2001. Magnetic stability of oceanic gabbros from ODP Hole 735B. Earth Planet. Sci. Lett. 193, 287–302.

York, D., 1966. Least squares fitting of a straight line. Can. J. Phys. 44, 1079.

Please cite this article as: Baines, A.G., et al., The rate of oceanic detachment faulting at Atlantis Bank, SW Indian Ridge Earth and Planetary Science Letters (2008), doi:10.1016/j.epsl.2008.06.013